Electronic structure of Mg: From monolayers to bulk

F. Schiller,[1,*] M. Heber,[1,2] V. D. P. Servedio,[1,3] and C. Laubschat[1]
[1]*Institut für Festkörperphysik, TU Dresden, 01062 Dresden, Germany*
[2]*Freudenberg Dichtungs-und Schwingungstechnik KG, 69465 Weinheim, Germany*
[3]*Sezione INFM and Dipartimento di Fisica, Università "La Sapienza," Piazzale Aldo Moro 2, 00185 Roma, Italy*
(Received 4 June 2003; revised manuscript received 26 January 2004; published 15 September 2004)

The structure of thin Mg films epitaxially grown onto a W(110) crystal was analyzed by low energy electron and Auger electron diffraction verifying a growth of bulk Mg. Normal-emission angle-resolved photoemission spectra of the growing films reveal quantum well states on both sides of a surface state. These states result from electron confinement in the Mg layer and are used to derive the electronic structure perpendicular to the surface. Off-normal, the electronic structure is dominated by the parabolic dispersion of surface states forming circles around the $\bar{\Gamma}$-points and ellipses around the $\bar{M}$-points in the Fermi surface cuts.

DOI: 10.1103/PhysRevB.70.125106 PACS number(s): 61.14.−x, 71.15.−m, 71.18.+y, 71.20.Dg

I. INTRODUCTION

The electronic structure determines most properties of the materials. Different theoretical approaches have been used to determine the band structure, however, often they are limited not only by the approximations used but also by the lack of available experimental data to verify their applicability. The standard experimental technique to study the occupied electronic structure is angle-resolved photoelectron spectroscopy (photoemission, PE), where energy and momentum (wave-vector) of emitted photoelectrons are analyzed. In a simple interpretation, one usually compares the experimentally derived binding energies to the calculated electronic ground state energies, neglecting the fact that the photoemission process leaves the atom in an excited state. Particularly in narrow-band systems severe discrepancies may arise between results of band-structure calculations and experiment, and it is difficult to decide whether the disagreement is caused by improper consideration of electron correlation in the initial state or by final state effects like electron-hole pair creation and incomplete screening. For wide-band systems like Mg metal, on the other hand, final state effects may be expected to be weak, and possible deviations of the experimental results from the predictions of theory may be related to the initial state. A second problem of the experimental technique lies in the fact that due to the violation of translational symmetry perpendicular to the sample surface only the parallel component of the wave vector is conserved and further assumptions have to be made to deduce the value of the perpendicular component, $k_\perp$, from the experimental data.[1] During the last years the analysis of quantum well states (QWS) arising in thin epitaxial films has been found suitable to investigate the band structure perpendicular to the surface not involving the $k_\perp$-problem.[2]

The valence states of the so-called free electronlike metals Be, Mg, and Al as well as the *sp*-like electrons of the noble metals Cu, Ag, and Au represent the most ideal candidates for metallic bonding. The electronic structure of these materials, however, is not totally free-electronlike, as can be concluded from the energy gaps in the band structures usually populated by surface states. Among the alkaline earth-metals Be and Mg are best studied, the first due to its anomalous physical properties,[3,4] the latter as an *ideal* hexagonal closed-packed lattice with simple electronic structure. While earlier photoemission experiments on Mg single-crystals found the electronic structure dominated by surface state emissions,[5,6] recent work on thin Mg films grown on Si(111) gave evidence of QWS derived from bulk *sp*-bands.[7]

In this report we present a study of both the crystalline and electronic structure of thin epitaxial films of Mg metal grown on a nonreactive W(110) surface. The growth of Mg on the W(110) crystal was studied by low-energy electron diffraction (LEED) in order to derive information about the long range order and the crystalline structure parallel to the surface, and by Auger electron diffraction (AED) in the forward scattering mode for the short range order and the lattice constant perpendicular to the surface.

Angle-resolved photoemission experiments were performed to determine the electronic structure, and the results were compared to Layer Korringa-Kohn-Rostoker (LKKR) and full potential local orbital calculations. In Sec. IV we will show that Mg grows in hcp bulk structure on W(110) with the basal (0001)-plane parallel to the surface. In Sec. V the QWS observed in thin Mg films are analyzed in the framework of a simple phase accumulation model (PAM) and from the results the band structure perpendicular to the Mg(0001) surface is derived. An analysis of the electronic structure of thick Mg-films gives further insight to band structure and Fermi-surface and is presented in last part of Sec. V.

II. EXPERIMENTAL DETAILS

Photoemission experiments were performed using a high-resolution angle-resolved hemispherical analyzer (SCIENTA 200), a monochromatic high-intensity He-discharge lamb (Gammadata VUV 5000) using mainly photon energies of $h\nu$=21.2 eV (He Iα), 23.1 eV (He Iβ), 40.8 eV (He IIα), and 48.4 eV (He IIβ), and a monochromatic Al-K_α x-ray source (1486.65 eV). The total system energy resolution was set to 50 meV ($h\nu<50$ eV) and an angular resolution of 1°

was chosen. The W(110) substrate was mounted on a six-axis manipulator allowing apart from translation three independent rotations of the sample (polar angle θ, azimuthal angle φ, and tilt angle α).

The W(110) crystal was cleaned by heating (1200 K) in O_2 (10^{-5} Pa) for about 20 min followed by several sample flashes to 2300 K for 5 s, until a very sharp $p(1\times1)$ LEED pattern with low background emissions indicated a clean and well ordered surface. Mg films were prepared at room temperature by electron-beam deposition from a Ta-crucible that was carefully outgased prior to experiments. The base pressure was 6×10^{-9} Pa and did not exceed the 10^{-8} Pa-region during Mg deposition. The deposition rate was tuned to 3.7 monolayers (ML) per minute as checked by means of a quartz microbalance, core level photoemission (Mg2*s* vs W4*f* core-levels) and quantum-well state behavior (see below). Cleanliness was checked by the absence of any impurity core-level emission in x-ray PE spectra and absence of oxygen and carbon valence band features in ultraviolet PE. The prepared Mg-films were found to be not reactive revealing no changes of the PE spectra for longer periods.

III. THEORETICAL APPROACH

The LKKR method has proven to be an effective tool for calculating photoemission spectra in the frame of the one-step-model.[8] The use of the Green's function formalism allows us to introduce finite lifetime effects (line broadening) by direct access to the imaginary part of the self-energy and to perform calculations for a semi-infinite crystal. In our specific case, the muffin-tin scattering potential of the Mg atoms in the crystal was generated by a self-consistent linear muffin-tin orbital program relying on the local density approximation of the density functional theory. The energy dependent self-energy of the occupied and unoccupied states, the geometry of the surface potential barrier (potential in the region between the crystal and the vacuum), as well as the previously calculated muffin-tin potentials, constitute together with the parameters of the experimental set up (direction of polarization vector, photon energy) the input information of our LKKR calculation. The energy position of surface states depends strongly on the surface potential barrier that was modeled by a step function placed at 47% of the bulk nearest neighbor distance above the surface. Although such a step function is a crude approximation if the calculation of unoccupied surface states is concerned, it presents a good description of the surface potential below the Fermi energy where the influence of the $1/r$ dependence of the image potential is negligible.[9,10]

FPLO (Ref. 11) on the other hand is an accurate band structure calculation program based on the linear combination of atomic orbital method. The Kohn-Sham Bloch states of the crystal are expanded in terms of nonorthogonal atomiclike orbitals. The atomic orbitals which overlap and form the valence bands are calculated as a function of a compression parameter. At each self-consistent cycle, not only the effective potential is recalculated but also this set of compression parameters (one for each orbital in the valence states) is optimized to minimize the total energy. This trick reduces the number of atomic orbitals needed to describe valence bands in solids.[12] In our case only the $2s2p3s3p$ orbitals of Mg were used together with a mesh of $15\times15\times15$ points in the reduced Brillouin zone.

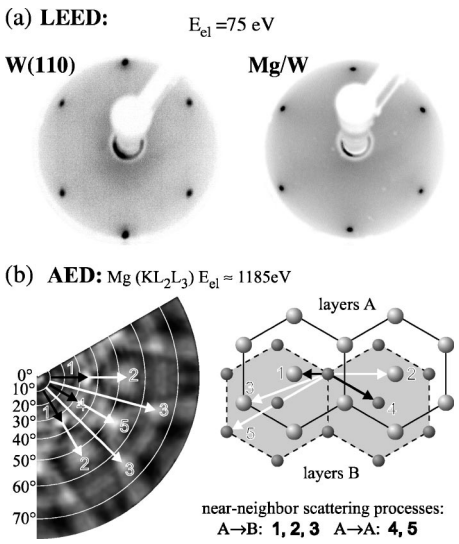

FIG. 1. (a) Comparison of the LEED pattern of a W(110) (left) and a 60 ML Mg/W(110) surface (right-hand side), respectively. (b) Two-dimensional Auger-electron diffraction pattern in stereographic projection of a 60 ML Mg/W(110) film. Light colors are used for high intensity. Theoretically expected positions of intensity enhancement are indicated in the model and verified in the AED pattern.

IV. GROWTH OF Mg/W(110)

The W(110) surface has been demonstrated to be an ideal substrate for the epitaxial growth of several fcc(111) and hcp(0001) materials. The W(110) face is well-closed as compared to other surfaces and represents a squished hexagon allowing hexagonal growth without large distortion. In the case of the Mg(0001) ($a=3.21$ Å) and W(110) ($a=3.16$ Å) the lattice mismatch in one direction amounts to only 1.6%.[13]

Above 3 monolayers Mg grows in a layer-by-layer mode as observed by sharp quantum-well-features and the absence of QWS mixing which is observed if terraces of different heights are present[2] (see below). The LEED pattern of the thinnest overlayer investigated (3.7 ML) showed already additional hexagonal spots to the W(110) substrate indicated by several sharp points in the LEED pattern along the $[\bar{1}10]$-direction. For thicker Mg layers only sharp hexagonal LEED patterns were obtained. Figure 1(a) shows the LEED pattern of the W(110) substrate and a 60 ML thick Mg film for an electron energy of 75 eV. Comparison of the spot distances reveal a lattice constant of $a=b=(3.25\pm0.07)$ Å. No thickness-dependent alteration of the LEED pattern was found.

Auger electron diffraction (AED) experiments were utilized to extract information about the lattice constant perpendicular to the surface. In this experiment forward scattering of the Mg-KL_2L_3 Auger-electrons (^1D, electron energy

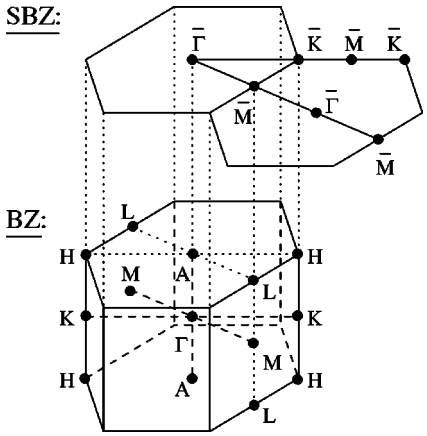

FIG. 2. Brillouin zone and the corresponding (0001) surface Brillouin zone of a hexagonal lattice.

1185 eV) was used giving rise to Auger electron diffraction (AED).[14,15] In a very simple picture, high-energetic electrons ($E_{\mathrm{kin}} \geqslant 500$ eV) emitted from the atomic core are scattered by the positive cores of neighboring atoms which leads to intensity increases along the respective directions. In our case, we used the Mg-KL_2L_3 Auger-electron decay of the structurally rich *KLL*-Auger spectra[16] due to its high intensity compared to the Mg2*s* and 2*p* core-level PE signals. The Mg1*s* PE signal was not used in order to avoid large contributions of backscattered electrons. The Auger-emission spectra were taken in a polar angle range of 120° and in an azimuthal angle range of 75° (approx. 6000 spectra). The spectra were normalized by subtracting the background from the peak intensity and dividing the difference by the background on the high-kinetic energy side of the peaks. This results in a normalized two-dimensional intensity distribution as shown in Fig. 1(b) in a stereographic projection, where light colors represent high and dark areas low intensity. All main diffraction spots expected for hexagonal stacking are observed. From the angular positions of the diffraction spots and the knowledge of the lattice constant parallel to the surface, derived from the LEED experiment, the Mg lattice constant perpendicular to the surface was determined as $c=(5.25\pm0.14)$ Å.

A comparison of the experimentally derived lattice constants of the grown films with the lattice constants of hexagonal Mg ($a=b=3.21$ Å, $c=5.21$ Å) (Ref. 13) suggests the growth of bulk Mg onto the W(110) substrate within experimental error.

V. BAND STRUCTURE RESULTS AND DISCUSSION

A. Quantum well state analysis

The reciprocal lattice of a hexagonal structure like Mg is again hexagonal and also its Brillouin zone. The three-dimensional Brillouin zone and the two-dimensional surface Brillouin zone (SBZ) of the (0001) surface are shown in Fig. 2.

Photoemission spectra taken with several photon energies in normal emission geometry for a 22 ML thick Mg/W(110) film are shown in Fig. 3 probing bands along the perpendicular ΓA direction. None of the observed peaks shows dispersion along the ΓA direction suggesting a two-dimensional character. Comparison with earlier PE experiments on bulk Mg (Refs. 5 and 6) assign the strong emission at approx. −1.6 eV to the $\bar{\Gamma}$ surface state while the other structures were not observed for bulk samples. Further information about these emissions can be obtained taking PE spectra for different thicknesses. A respective series of PE spectra recorded in normal emission geometry and with a 40.8 eV photon energy is shown in Fig. 4 for overlayer thicknesses up to 81 ML. While the surface state remains nearly unaffected the additional emissions change their energetic positions with the thickness and are thus identified as quantum well states or resonances of the Mg bulk bands in ΓA direction. Such states are formed due to the confinement of the electrons in the Mg film perpendicular to the surface. The electron is (at least partially) reflected on both sides of the film, at the Mg/vacuum side and the Mg/W(110) interface. PE spectra were taken every 3.7 ML (corresponding to 1 min deposition time) where the thickness was determined afterwards by analyzing the intensity variation at the Fermi level: From the FPLO calculation it can be concluded that the upper branch of the bulk *sp* band runs through 26% of the Brillouin zone therefore every $1/0.26=3.85$ lattice constants equal to 7.7 ML a new QWS should occur.[7] The QWS can be observed up to 81 ML (the largest thickness investigated). Normal emission PE experiments of W(110) show that the Γ-Σ-N direction is characterized by an energy gap between −6.3 eV and −3.4 eV with respect to E_F built up by the Σ_5^1

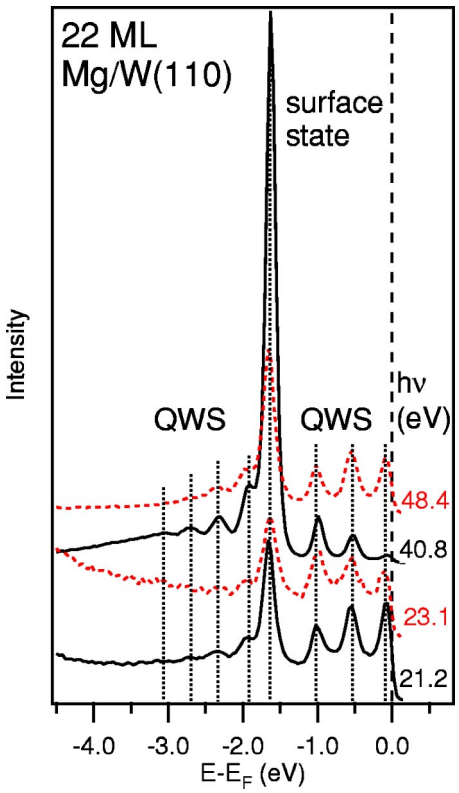

FIG. 3. (Color online) Normal emission photoemission spectra for a 22 ML Mg/W(110) film taken at several photon energies.

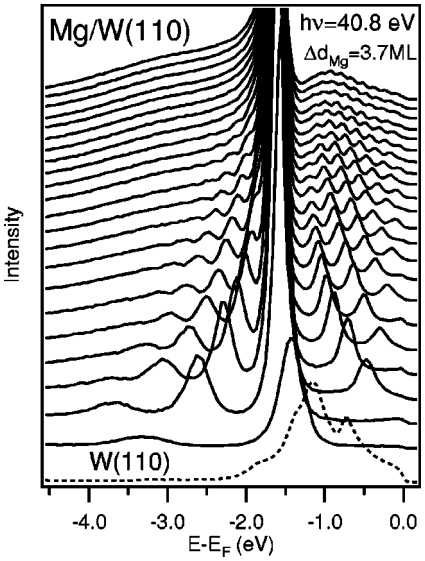

FIG. 4. Normal emission photoemission spectra of a growth series of Mg/W(110) taken at 40.8 eV photon energy.

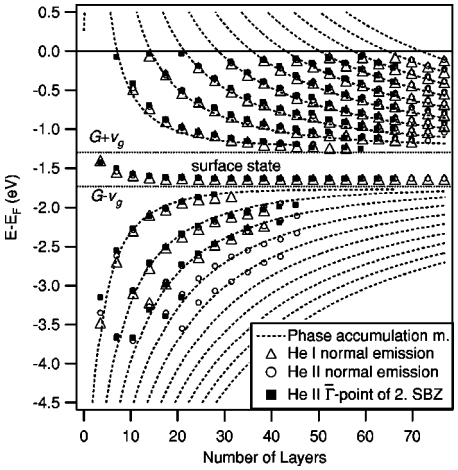

FIG. 5. Energy diagrams of quantum-well states as a function of film thickness. The experimental data were obtained at the $\bar{\Gamma}$-points of the first and second Brillouin zones measured at $h\nu=21.2$ eV and 40.8 eV. The dashed lines connecting the experimental points represent the best fit using the phase accumulation model and the standard two band model.

and the Σ_5^2 states in relativistic double-group notations.[17,18] In this energy region Mg electronic states of Δ_2 symmetry (nonrelativistic single-group notation) are totally confined and are called quantum well states. As indicated in Figs. 3 and 4, however, states exist also for energies between −3.4 eV and the Fermi energy. In this region partial reflection of the wave function is caused by symmetry differences to the substrate wave function or differences in crystal parameters.[2,19] The respective states are called quantum well resonances. For simplicity in this work we will state QWS for both types of electron confinement. For the upper branch of the *sp* band similar QWS were recently observed up to a thickness of 44 ML Mg for low temperature growth of Mg on Si(111).[7] In contrast to this previous work, however, the change of the energy position of the QWS with the layer thickness are observed in the present case on both sides of the band gap showing that individual QWS shift toward the edges of the band gap when increasing the overlayer thickness. Furthermore, in contrast to the Si(111) substrate, on W(110) Mg grows epitaxially at room temperature even for large thicknesses.

The QWS states were analyzed in the framework of a simple phase accumulation model.[20,21] Here, the metallic film is considered as a quantum well perpendicular to the surface confining electrons between the substrate and vacuum. Only such $k_\perp$ values of the electrons are allowed that fulfill the stationary state condition for integer n,

$$2k_\perp d + \Phi_B + \Phi_C = 2\pi n, \tag{1}$$

where Φ_B and Φ_C are the phase shifts at the Mg-W interface and at the Mg-vacuum side. The film thickness is $d=Nc/2$, where N describes the number of monolayers along the surface normal, and c is the lattice constant ($c/2$ is used to account for 2 atoms in the hexagonal unit cell). The phase shift on the vacuum side is given by[22]

$$\Phi_B = \pi\left(\sqrt{\frac{3.4\,\mathrm{eV}}{E_V - E}} - 1\right), \tag{2}$$

where E_V is the vacuum level that is related to the experimentally observed Fermi level E_F by $E_V=E_F+W_{\mathrm{Mg}}$ with the Mg work function $W_{\mathrm{Mg}}=3.66$ eV. The phase shift on the substrate side Φ_C is calculated by

$$\Phi_C = 2\ \arcsin\sqrt{\frac{E - E_L}{E_U - E_L}} - \pi, \tag{3}$$

where E_U and E_L denote the energies of the upper and lower edges of the W band gap along $\Gamma-\Sigma-\mathrm{N}$,[23,24] respectively, taken from Ref. 18. Finally, $k_\perp$ was obtained from a standard two-band nearly-free-electron approach, solving the determinant

$$\begin{vmatrix} (\hbar^2/2m)k_\perp^2 - E & v_G \\ v_G & (\hbar^2/2m)(k_\perp - G)^2 - E \end{vmatrix} = 0 \tag{4}$$

with the magnesium reciprocal lattice vector G, the respective Fourier-coefficient of the crystal potential, v_G (width of the band gap $\approx 2v_G$), and the electron mass m. E as well as E_U, E_L, and the midgap position $E_G=\hbar^2G^2/2m$ are taken positive and measured from the bottom of the valence band $-E_V$. A fit of all data-points from Fig. 4 to the theory described above turned out to be very sensitive to the values of G, v_G, and the vacuum level E_V. From the fit $E_G=E_F-(1.51\pm0.03)$ eV and $v_G=(0.28\pm0.03)$ eV are derived and the results are shown in Fig. 5. Inclusion of a further phase shift Φ_{scatt} that accounts for a possible band coupling of substrate and overlayer bands outside the substrate band gap[25,26] gave worse results suggesting that such an additional phase shift does not take place. This in turn indicates weak coupling of Mg and W bands. The fitted vacuum level position $E_V=(10.55\pm0.03)$ eV allows to determine the binding energy of the bottom of the valence band, $\Gamma_1^+=E_V-W_{\mathrm{Mg}}$

TABLE I. Binding energy positions (in eV) of the Mg band structure at Γ. The error bars include the errors of the fit and the experimental resolution.

	Expt.	Expt.[a]	FPLO	Tight binding[b]
Γ_1^+	6.89±0.06	6.15±0.1	6.94	6.89
Γ_3^+	1.79±0.09	1.7±0.1	1.69	1.81
Γ_4^-	1.23±0.09	0.9±0.1	1.30	1.51

[a]From Ref. 6.
[b]From Ref. 27.

$=(6.89\pm0.03)$ eV, and together with G and v_g, the band gap binding energies $\Gamma_3^+=(1.79\pm0.09)$ eV and $\Gamma_4^-=(1.23\pm0.09)$ eV. Table I compares these values to experimental data from Ref. 6, theoretical values from our FPLO calculations, and recent data from Ref. 27.

Differences are found between the experimental data of Ref. 6 obtained from direct PE experiment and the data presented here derived by the quantum-well analysis. We attribute these differences to the width of the bulk states measured in the direct PE experiment that make a precise determination of the energy position difficult. Note that QWS on both sides of the overlayer band gap are described within our model by the same parameter values. The good accordance of the two-band model with our FPLO calculation and the experimental data obtained by the phase accumulation model is illustrated in Fig. 6. For a better presentation the first band along ΓA (Δ_1) of the FPLO calculation is backfolded around the A-point.

From a closer inspection of Figs. 4 and 5 it is evident that the binding energy of the surface state increases slightly with

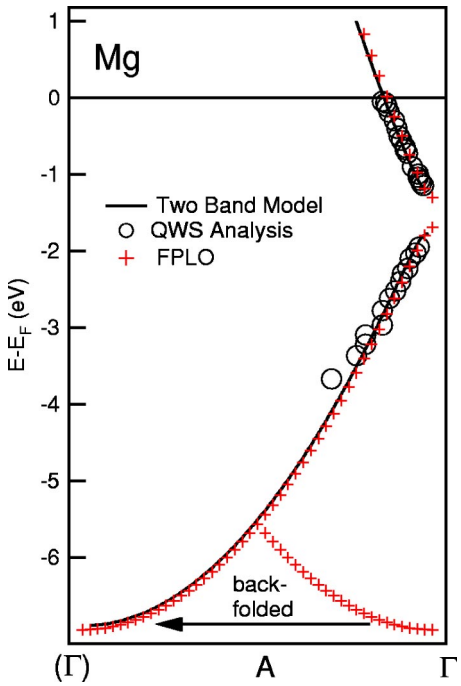

FIG. 6. (Color online) Band dispersion along ΓA-direction from the experimental points derived by the PAM, the two-band model, and the FPLO code.

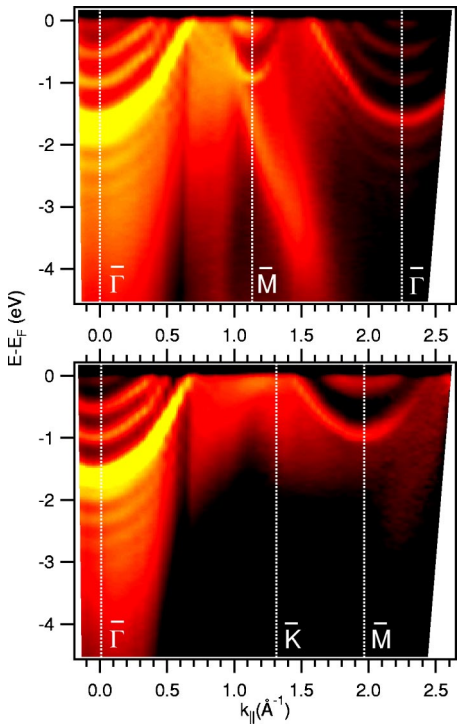

FIG. 7. (Color online) Intensity distribution plots of 22 ML Mg/W(110) along $\overline{\Gamma M}$ (top) and $\overline{\Gamma K}$ (bottom) directions, respectively. Shown is the logarithmic PE intensity by a color scale, where light colors define high intensity ($h\nu=40.8$ eV).

film thickness reaching a constant value of (1.63 ± 0.06) eV above 12 ML. This behavior is attributed to a perturbation of the wave-function if the decay length is lower than the film thickness.[7]

The form and width of the quantum well states varies with the thickness of the Mg film (see Fig. 4). A similar behavior was observed for the Au/Fe(100) system and interpreted by

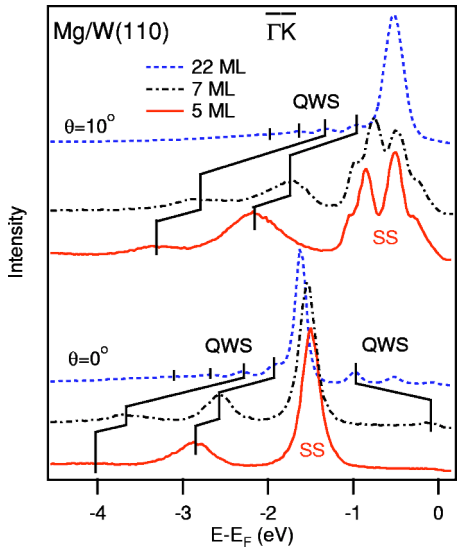

FIG. 8. (Color online) PE spectra of the region of the surface state and the quantum well states taken in normal emission geometry and at $\theta=10°$ ($k_\parallel^f=0.55$ Å^{-1}) for Mg films of different thicknesses.

considering not only the initial but also the final state of the photoemission process including quasiparticle lifetimes.[28,29] The intensity of the quantum well states additionally varies with the photon energy as observed in Fig. 3 and is also related to the final state.[30,31]

For further characterization of the electronic structure of Mg, PE spectra were additionally taken in off-normal emission. Experimental data along the $\overline{\Gamma M}$ and $\overline{\Gamma K}$ directions for a 22 ML thick Mg-film is shown in the form of an intensity plot in Fig. 7 with a logarithmic intensity scale to enhance minor features. The intensity of the surface state at the $\overline{\Gamma}$-point is very intense and cannot be separated from the first QWS of the lower band branch. Both the surface state and the QWS's reveal parabolic dispersion in both high symmetry directions. A least-squares fit results in an effective electron mass of $m^*=(1.02\pm0.02)\ M_e$, with M_e being the free electron mass. Along the $\overline{\Gamma M}$ direction almost identical surface state and QWS-emissions are observed at the $\overline{\Gamma}$ points of the first and second surface Brillouin zone. For surface states such a behavior is expected, however, QWS of the same energy positions and the same dispersion relation only occur if the boundary conditions to the tungsten substrate are similar at both Mg$\overline{\Gamma}$-points that do not correspond to the W(110)-$\overline{\Gamma}$-points. A further structure that can be observed is an additional surface state around the $\overline{M}$-point that reveals also a parabolic dispersion. Similar to the $\overline{\Gamma}$ surface state, it is observed close to the bottom of the energy gap at (0.95 ± 0.05) eV residing (0.17 ± 0.05) eV above the lower band edge. The remaining structures are interpreted as bulk bands.

An additional interesting phenomenon are *k*-dependent splittings of the surface state that occur at low Mg coverages and may be described by the coexistence of electron states with different effective masses. The effect is illustrated in Fig. 8 for PE spectra of several film thicknesses along the $\overline{\Gamma K}$ direction. While at the $\overline{\Gamma}$-point the surface-state signal consists of a single line it reveals a splitting into at least 4 components for an emission angle of $10°$ ($k_{\parallel}^{f}=0.55$ Å^{-1}). The magnitude of the splitting decreases with increasing thickness of the Mg layer. For coverages exceeding 12 ML the individual components are not longer resolved spectroscopically, but a broadening of the surface state signal with respect to the linewidth observed for thick Mg films points to the presence of a respective substructure at even larger coverages. We ascribe this phenomenon to the lattice mismatch between the Mg film and the underlying W substrate that may lead (i) to distortions of the surface geometry and (ii) variations of the confinement conditions at the Mg/W interface that reveal a periodicity different from that of the Mg

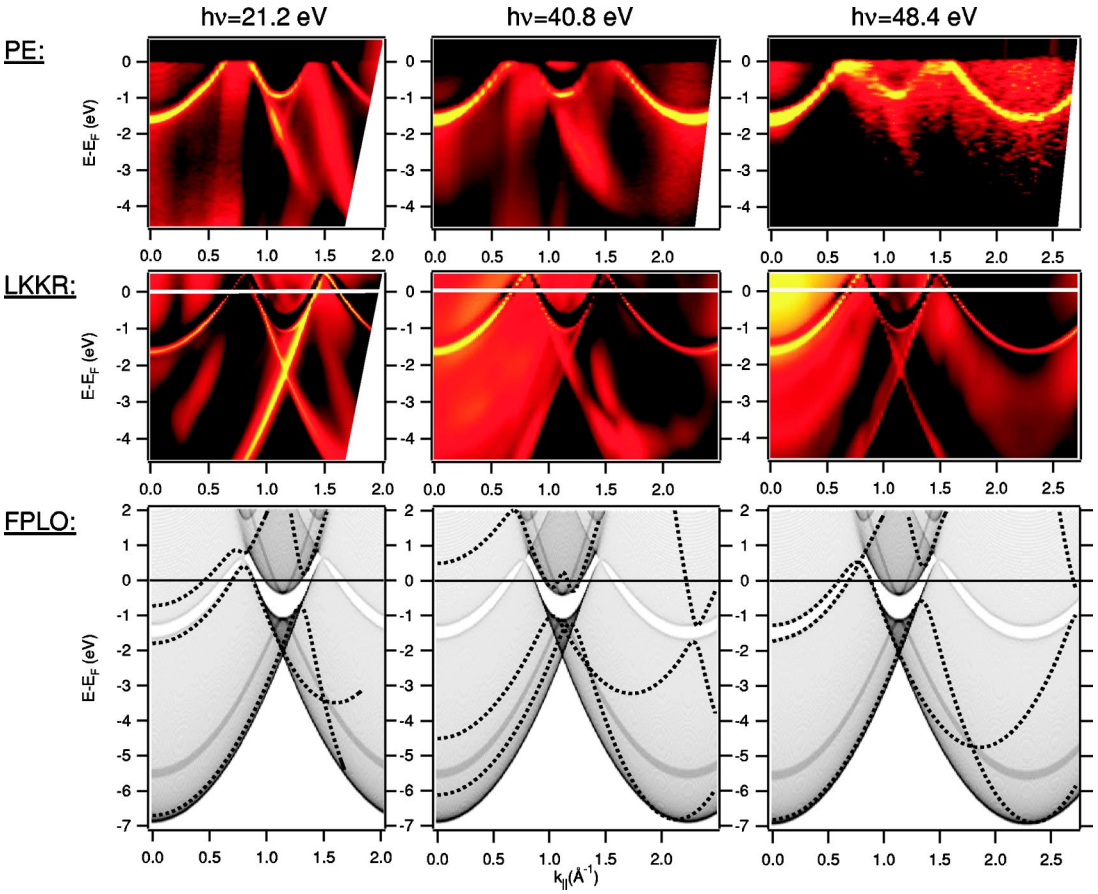

FIG. 9. (Color online) Intensity distribution plots of a 60 ML Mg/W(110) film along $\overline{\Gamma M}$ direction measured in a photoemission experiment and calculated by the LKKR method. At the bottom, the bulk band structure of Mg is shown as obtained from a FPLO calculation projected along the (0001) direction (grey areas). Dotted lines visualize the bulk band dispersion assuming free-electronlike final states.

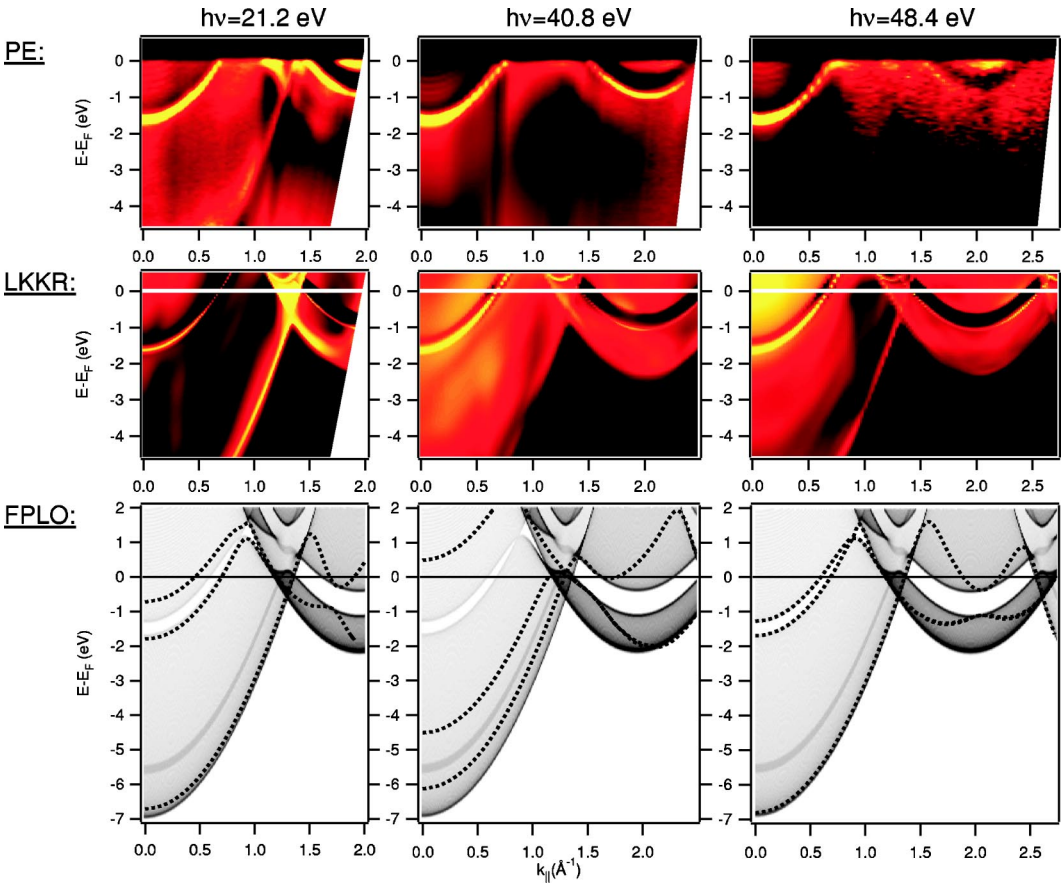

FIG. 10. (Color online) Intensity distribution plots of a 60 ML Mg/W(110) film along $\overline{\Gamma K}$ direction measured in a photoemission experiment and calculated by the LKKR method. At the bottom, the bulk band structure of Mg is shown as obtained from a FPLO calculation projected along the (0001) direction (grey areas). Dotted lines visualize the bulk band dispersion assuming free-electronlike final states.

lattice. Both mechanisms may lead to splittings of the surface state, a proper theoretical analysis of the phenomenon, however, demands detailed studies of the crystallographic structure in the low coverage regime and is beyond the scope of the present work.

B. Mg bulk electronic structure

The surface band structure of Mg single-crystals has been subject to earlier photoemission studies.[5,6] In both studies the PE spectra were found to be characterized by surface state emissions and additional broad and usually low intense bulk emissions. A similar behavior is observed here for thick, bulklike films. The electronic structure of a 60 ML Mg/W(110) film along the two high symmetry directions $\overline{\Gamma M}$ and $\overline{\Gamma K}$ as measured by angle-resolved PE and calculated by LKKR one-step PE calculations assuming a semi-infinite Mg crystal is shown in Figs. 9 and 10 as density plots, respectively. As before a logarithmic intensity scale is used for the color in order to strengthen weaker emissions. In addition, a FPLO calculation of the projected band structure (projected along [0001]-direction) of Mg is shown by shaded areas superimposed by the calculated bulk band dispersion assuming free electron final states (dotted lines) using

$$\boldsymbol{k}_{\parallel}^{f} = \sqrt{\frac{2m^*}{\hbar^2}} \cdot \sqrt{E_{\mathrm{kin}}} \cdot \sin\theta \cdot \begin{pmatrix} \sin\varphi \\ \cos\varphi \end{pmatrix}, \tag{5}$$

$$k_{\perp}^{f} = \sqrt{\frac{2m^*}{\hbar^2}} \cdot \sqrt{E_{\mathrm{kin}} \cdot \cos^2\theta + V_0}, \tag{6}$$

where $V_0 = -E_V = 6.94$ eV denote the inner potential, $m^* = 1.02 \cdot M_e$ the effective electron mass (M_e the electron mass), and $E_{\mathrm{kin}} = h\nu - W_{\mathrm{Mg}} - E_B$ the kinetic energy depending on the photon energy $h\nu$, Mg work function W_{Mg}, and the binding energy E_B.

At $\overline{\Gamma}(k_{\parallel}=0)$ the surface state is found experimentally at (1.63 ± 0.03) eV binding energy and is the most prominent feature observed at the photon energies used ($h\nu = 21.2$ eV, 40.8 eV, 48.4 eV). It disperses parabolically towards the Fermi level E_F when increasing the emission angle crossing E_F at $k_{\parallel} = 0.6$ Å^{-1} for both $\overline{\Gamma M}$ and $\overline{\Gamma K}$ high symmetry directions. At larger emission angles it is also possible to observe contributions of a surface state in the $\overline{M}$ band gap as well as less intense features arising from bulk bands. Experimentally all the surface states are found close to the bottom of the bulk band gap in agreement with the LKKR results. Also the bulk emissions agree quite well with the expectations based on LKKR and FPLO calculations. Small deviations, seen for example for one bulk band along $\overline{\Gamma M}$ direction measured at 21.2 eV photon energy and $k_{\parallel} > 1.5$ Å^{-1}, are attributed to final states effects already found for bulk Mg at low photon

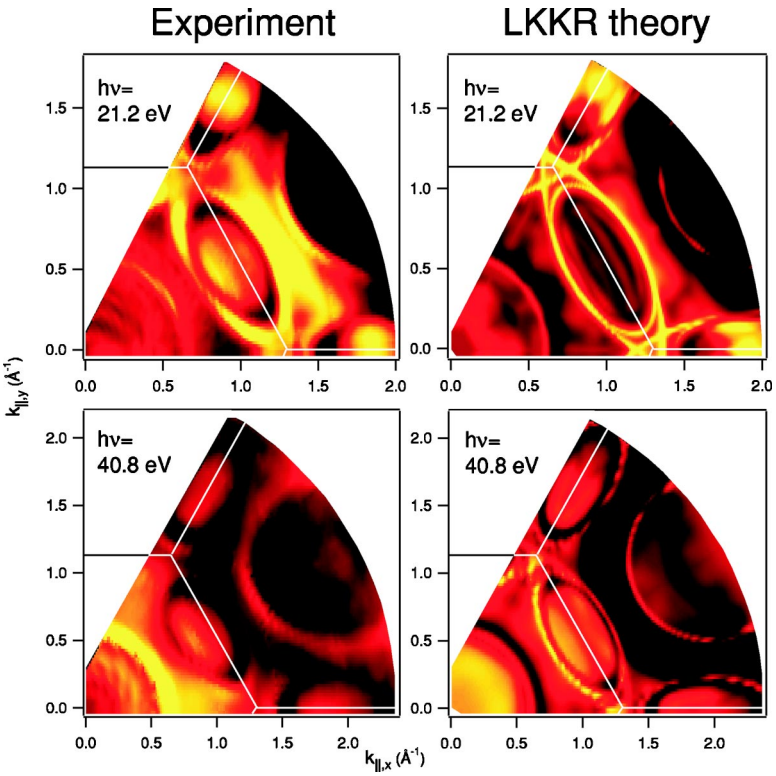

FIG. 11. (Color online) Fermi surface maps measured by photoemission and calculated by the LKKR method for 21.2 eV and 40.8 eV photon energies, respectively.

energies.[6] Comparison of the LKKR photoemission calculation and the FPLO projected band structure reveal bulk emissions everywhere except within the band gaps. These band emissions can be attributed to density of state like emissions.

If for a given kinetic energy the PE signal is recorded as a function of wave-vector the spatial intensity distribution is mapped. If the kinetic energy is equal to the Fermi energy, this intensity distribution represents basically a cut through the Fermi surface including, however, also other effects like emissions from surface states, density-of-states like contributions,[32] and PE diffraction. Nevertheless, such plots often are referred as Fermi energy cuts. Figure 11 shows such Fermi surface cuts measured and calculated for 21.2 eV and 40.8 eV photon energies, respectively. The calculation is based on the LKKR method that allows apart from bulk contributions the proper consideration of surface state emissions. The $\overline{\Gamma K}$-direction represents the *x*-axis. The surface state that crosses E_F at 0.6 Å^{-1} in $\overline{\Gamma K}$ and $\overline{\Gamma M}$ directions becomes a ring around $\overline{\Gamma}$ and can be observed both in the first and second SBZ. Another interesting detail of the plots are intense elliptic structures around the $\overline{M}$-points that are derived from the surface state also visible in the PE spectra presented in Figs. 9 and 10. Further contributions in the Fermi surface cuts come from direct bulk emissions and to less extent the still visible QWS emissions around the $\overline{\Gamma}$-points.

VI. CONCLUSIONS

We have shown by a combined study of low-energy electron and Auger-electron diffraction that Mg forms single-crystalline films with (0001)-orientation on W(110) and lattice constants corresponding to bulk Mg. Angle-resolved PE spectra taken at photon energies between 20 and 50 eV are characterized by surface state and quantum-well-state emissions. From the analysis in the framework of a simple phase accumulation model the band dispersion perpendicular to the surface (ΓA-direction) was derived that is in excellent agreement with results of FPLO band-structure calculations. Surface state emissions also dominate the angular dispersive intensity plots at the Fermi energy. They form circles around the $\overline{\Gamma}$-points and ellipses around the $\overline{M}$-points in agreement with results of PE calculations in the framework of LKKR.

*Electronic address: schiller@physik.phy.tu-dresden.de

[1] E. W. Plummer and W. Eberhardt, Adv. Chem. Phys. **49**, 533 (1982).
[2] T.-C. Chiang, Surf. Sci. Rep. **39**, 181 (2000).
[3] M. Y. Chou, P. K. Lam, and M. L. Cohen, Phys. Rev. B **28**, 4179 (1983).
[4] E. W. Plummer and J. B. Hannon, Prog. Surf. Sci. **46**, 149 (1994).
[5] U. O. Karlsson, G. V. Hansson, P. E. S. Persson, and S. A. Flodström, Phys. Rev. B **26**, 1852 (1982).
[6] R. A. Bartynski, R. H. Gaylord, T. Gustafsson, and E. W. Plummer, Phys. Rev. B **33**, 3644 (1986).

[7] L. Aballe, C. Rogero, and K. Horn, Phys. Rev. B **65**, 125319 (2002).
[8] J. B. Pendry, Surf. Sci. **57**, 679 (1976).
[9] S. Loebus, R. Courths, S. V. Halilov, H. Gollisch, and R. Feder, Surf. Rev. Lett. **3**, 1749 (1996).
[10] V. D. P. Servedio, S.-L. Drechsler, and T. Mishonov, Phys. Rev. B **66**, 140502 (2002).
[11] K. Koepernik and H. Eschrig, Phys. Rev. B **59**, 1743 (1999).
[12] H. Eschrig, *Optimized LCAO Method* (Springer, Berlin, 1989).
[13] W. P. Pearson, *A Handbook of Lattice Spacing and Structures of Metals and Alloys* (Pergamon, Oxford, 1967).
[14] W. F. Egelhoff, Jr., Crit. Rev. Solid State Mater. Sci. **16**, 213 (1990).
[15] S. Chambers, Adv. Phys. **40**, 357 (1991).
[16] L. Ley, F. R. McFeely, S. P. Kowalczyk, J. G. Jenkin, and D. A. Shirley, Phys. Rev. B **11**, 600 (1975).
[17] R. H. Gaylord and S. D. Kevan, Phys. Rev. B **36**, 9337 (1987).
[18] J. Feydt, A. Elbe, H. Engelhard, G. Meister, C. Jung, and A. Goldmann, Phys. Rev. B **58**, 14 007 (1998).
[19] T. Miller, A. Samsavar, and T.-C. Chiang, Phys. Rev. B **50**, 17 686 (1994).
[20] P. M. Echenique and J. B. Pendry, J. Phys. C **11**, 2065 (1978).
[21] N. V. Smith, Phys. Rev. B **32**, 3549 (1985).
[22] E. McRae and M. Kane, Surf. Sci. **108**, 435 (1981).
[23] P. M. Echenique and J. B. Pendry, Prog. Surf. Sci. **32**, 111 (1989).
[24] N. V. Smith, N. B. Brookes, Y. Chang, and P. D. Johnson, Phys. Rev. B **49**, 332 (1994).
[25] A. M. Shikin, O. Rader, G. V. Prudnikova, V. K. Adamchuk, and W. Gudat, Phys. Rev. B **65**, 075403 (2002).
[26] A. M. Shikin, D. V. Vyalikh, G. V. Prudnikova, and V. K. Adamchuk, Surf. Sci. **487**, 135 (2001).
[27] H. J. Gotsis, D. A. Papaconstantopoulos, and M. J. Mehl, Phys. Rev. B **65**, 134101 (2002).
[28] J. J. Paggel, T. Miller, and T.-C. Chiang, Science **283**, 1709 (1999).
[29] J. J. Paggel, T. Miller, D.-A. Luh, and T.-C. Chiang, Appl. Surf. Sci. **162-163**, 78 (2000).
[30] A. Mugarza Ezpeleta, Ph.D. thesis, University of the Basque Country,
Spain, 2002.
[31] G. Neuhold, Ph.D. thesis, Freie Universität Berlin, Germany, 1996.
[32] M. Lindroos and A. Bansil, Phys. Rev. Lett. **77**, 2985 (1996).